

## Light transmissivity in the NESTOR site

E.G. Anassontzis<sup>a</sup>, P. Ioannou<sup>a</sup>, Chr. Kourkouvelis<sup>a</sup>, L.K. Resvanis<sup>a,\*</sup>, H. Bradner<sup>b</sup>

<sup>a</sup> *Physics Laboratory, University of Athens, Solonos 104, GR-10680 Athens, Greece*

<sup>b</sup> *Institute of Geophysics and Planetary Physics, Scripps Institution of Geophysics, University of California, La Jolla, California 92093-0225, USA*

Received 24 February 1994

The water transmissivity is a parameter of paramount importance in the design and construction of water Cherenkov detectors which are used as neutrino telescopes. The  $1/e$  transmission distance of 460 nm blue-green uncollimated light in deep sea-water (down to 4000 m) has been measured at three locations, in the NESTOR deployment site, off the coast of Pylos in South West Greece. The light path lengths were 7.44 m, 20.69 m and 40.37 m. The  $1/e$  transmission distance, for depths greater than 3500 m, is found to be  $55 \pm 10$  m.

### 1. Introduction

The field of neutrino astrophysics was born with the solar neutrino astronomy and the observation of neutrinos from Supernova 1987A. Since neutrinos are weakly interacting particles, they can travel extremely long distances before interacting. They can therefore convey information from very distant sources, while photons, especially in the TeV or high energy regime, get attenuated by interactions with the 3 K microwave and the infrared background.

A neutrino telescope can investigate a wide range of physics topics:

- High energy neutrino astronomy, namely detecting neutrinos which are produced by galactic e.g. X-ray binaries or extragalactic sources, such as the active galactic nuclei (AGNs);
- Neutrinos which are produced from the annihilation of dark matter particles;
- Neutrino oscillations, using neutrinos produced in the atmosphere;
- Neutrino oscillations, using a neutrino beam from a high energy particle accelerator.

The earth is transparent to neutrinos. In deep underwater neutrino telescopes the neutrinos are detected from the muons resulting from charged current neutrino interactions in the water. Muons can only be identified as neutrino induced if there is enough shielding of the detector from the cosmic ray muons. This is the reason for going deep underwater; the few kilometres of water above the detector act as a shield against the cosmic rays.

Presently there are four neutrino telescopes under construction: AMANDA in the South Pole ice at a depth of

about 1 km, BAIKAL at a depth of about 1 km in the Baikal lake, DUMAND at a depth of about 5 km off the coast of the big island of Hawaii and NESTOR, the European neutrino telescope at a depth of about 4 km off the coast of the South West of Greece. All four telescopes detect the Cherenkov light produced by the muons travelling in the water, with large photomultiplier tubes housed in pressure protective glass spheres. The muons – and the other relativistic charged particles – produce Cherenkov light in sea-water with a half cone angle of  $43^\circ$ . They emit about 250 Cherenkov photons per cm of particle path in the region of 300–500 nm where the phototubes are sensitive. Water transmissivity, in the same wavelength region, is a decisive parameter in the construction of a deep underwater neutrino detector. The spacing between the phototubes and thus the instrumented volume, the effective area of the detector, the rates of interesting events etc. are singularly influenced by the water transmissivity.

We are constructing NESTOR [1], which will be deployed off the coast of Pylos in the South West of Peloponnesos in Greece. As explained above it is very important to know accurately the transmissivity of light in sea-water and especially in the blue-green region where the quantum efficiency of the phototubes reaches its maximum value.

Usually the attenuation length of the light in water is measured in the laboratory, using water samples and well-collimated light beams with a path in water about 1 m long. In well-collimated beams, rays scattered more than about 0.01 rad are lost and the attenuation measured is due to the sum of absorption and scattering. Further, for clear water, the length of the water path in those instruments is short compared to the attenuation length of blue-green light, and large extrapolation must be made. In an experiment like NESTOR (or DUMAND [2]) the main light

\* Corresponding author.

attenuation mechanism is just the absorption since on the average as many photons will be scattered toward the photomultiplier as away from it (97% of all photons are propagated within a half-cone of  $5^\circ$  [3]). DUMAND and NESTOR are “poor geometry” experiments because they have a large angle of photon acceptance. For this reason, in designing DUMAND and NESTOR it is important only to know the absorption coefficient of blue-green light in sea-water. This is achieved readily using a transmissivity meter that can collect most of the scattered light, i.e. a “poor geometry” transmissivity meter. Bradner and Blackinton [4] measured, with a “poor geometry” transmissivity meter, the absorption of light in ocean water near the DUMAND site west of Keahole Point, Hawaii. They used a detector with variable length and uncollimated light path of 7.86 m and 84.00 m long. They used the term  $1/e$  transmission distance  $\beta$  to avoid confusion with the attenuation length, usually used in experiments with well collimated beams.

The same detector, with minor changes, was used by us on board the Russian Oceanographic vessel “Akademic Mstislav Keldish” in November of 1992 to measure the  $1/e$  transmission distance off the coast of Pylos in South West Greece, the site where NESTOR will be deployed.

## 2. Description of the instrument

The detector is a two part instrument, a wide-angle pulsed light source and the photodetector. The two parts are joined together with a variable length 3 mm diameter stainless steel wire (Fig. 1) and lowered into the sea with a hydrographic cable. The light source was emitting light in pulses and measurements of light intensities were made by the photodetector with different source–detector distances.

The light source is mounted on an aluminum frame which is hung at variable distances below the photodetec-

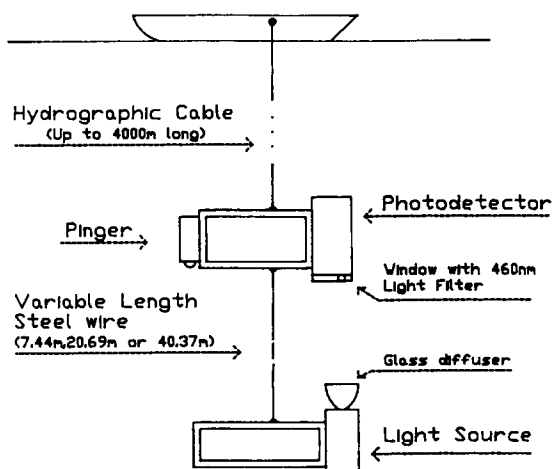


Fig. 1. Schematic diagram of the detector.

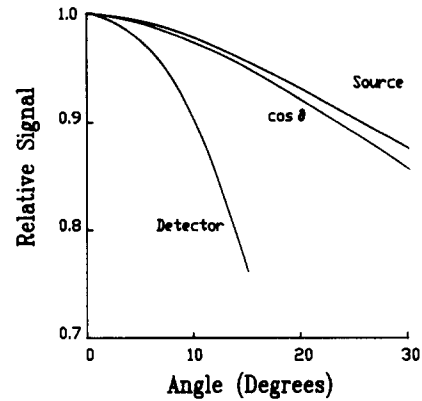


Fig. 2. Angular light intensity distribution of the light source and the angular acceptance of the photodetector (from Ref. [4]).

tor. It is a voltage-regulated commercial photostrobe (SUNPAK 411) in a 13 cm diameter cylindrical pressure case. The light source is set facing upwards and flashes every 30 s. A 23 cm diameter opal glass light diffuser is set in front of a commercial photoflood reflector. The light source produces the light intensity distribution in water shown in Fig. 2 (The figure is from Ref. [4]).

The photodetector is housed in a 20 cm diameter aluminum pressure tube with a conical Lucite window looking down. The angle acceptance of the photodetector is shown in Fig. 2 (the figure is from Ref. [4]). The light entering the window is filtered with a 460 nm interference filter and is detected by an EG&G model HUV 4000B photodiode that has an incorporated operational amplifier with an internal feedback resistor. To change the gain of the preamplifier, this internal feedback resistor could be changed by connecting in parallel an external feedback resistor through a special pressure bulkhead connector. The peak-value of the detected signal is held for a time of up to 4 s with a peak and hold circuit. The signal is digitized by a Burr Brown ADC80, tone-coded and transmitted to the shipboard through the hydrographic cable.

The digital signal on shipboard was split for monitoring on an oscilloscope, recorded on a magnetic tape and decoded to analog voltage. The analog voltage was recorded on a strip-chart recorder and monitored with a digital voltmeter.

## 3. Analysis of the data

The calculation of the  $1/e$  transmission distance is based on the comparison of the light intensities for two different distances between the light source and the photodetector. In a poor geometry experiment, the light intensity, due to the absorption, is assumed to decrease exponentially. Moreover the water can be assumed isotropic,

hence the light intensity (even without any absorption) decreases, by geometrical spreading, with the inverse square of the distance. Consequently, the light intensity from the initial value  $I_0$ , after transversing the short ( $S$ ) path or the long ( $L$ ) path is

$$I_S = I_0/S^2 \times e^{-S/\beta} \text{ and } I_L = I_0/L^2 \times e^{-L/\beta}, \quad (1)$$

where  $I_L$  and  $I_S$  are the corresponding light intensities on the photodetector and  $I_0$  is the light intensity of the light source;  $\beta$  as mentioned earlier is the  $1/e$  transmission distance.

From Eqs. (1) we can calculate the  $1/e$  transmission distance  $\beta$  as:

$$\beta = (L - S)/(\ln I_S/I_L - 2 \times \ln L/S). \quad (2)$$

During the measurements in the water, the peak-voltages  $V_L$  and  $V_S$  of the photodiode amplifier were recorded. The relationship between the output voltage of the photodetector and the detected light intensity was determined in the laboratory. This calibration was done in the air measuring isotropically emitted light which is attenuated with the inverse square of the distance of the source–detector. Special care was taken to avoid reflections from the floor or the walls around the photodetector. A 10% filter was used to attenuate the light from the light source to levels that were comparable to the levels achieved in the water for approximately the same distances and for the same gain feedback resistors. Then, by changing the distance between the light source and the photodetector, the light intensity received by the photodetector was reduced (by the inverse square of the distance) and the corresponding peak-voltage was recorded. In Fig. 3 these peak voltages are plotted versus the inverse square of the distance between the photodetector and the light source, i.e., versus different light intensities  $I$ , expressed in arbitrary units. Two different curves are shown corresponding to the two different gains used. The gain was set by an external feedback resistor on the preamplifier. From those calibration measurements of peak voltage versus light intensity

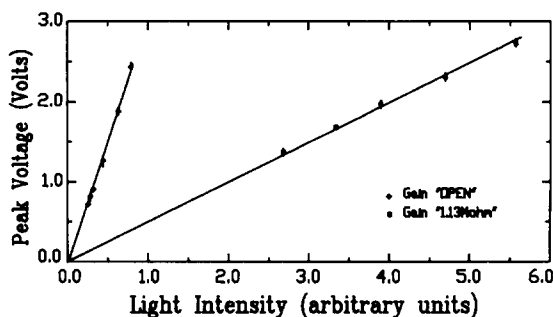


Fig. 3. Peak voltage versus the inverse square of the distance between the photodetector and the light source in the air (i.e. versus different light intensities expressed in arbitrary units).

(i.e. from Fig. 3) and from the ratio  $V_S/V_L$  as measured in the sea, the corresponding  $I_S/I_L$  was calculated and used in Eq. (2).

#### 4. Measurements in the sea

Measurements were made at various depths down to about 4000 m, using three different distances between the light source and the photodetector; 7.44 m, 20.69 m and 40.37 m. The gain was adjusted with two external feedback resistors; “open” (no external feedback resistor) and “1.13 M $\Omega$ ”. The depth of the photodetector was measured with an acoustic pinger attached on the photodetector frame and was checked by the length of the cable payed out. The difference between the photodetector depth as determined with the pinger and the cable payed out was less than 30 m, so the drift effect was minimal. Measurements were done in three different locations near the future NESTOR site, and at each depth a set of data were taken for 20 min:

Location “a”: 36° 37’N; 21° 34’E. The detector was lowered twice down to the maximum depth of 3650 m, each time with a different distance between the light source and the photodetector ( $S = 7.44$  m with “1.13 M $\Omega$ ” gain and  $L = 40.37$  m with “open” gain). The sea had a depth of about 3730 m. The drift of the ship was less than 0.2 knots.

Location “b”: 36° 29’N; 21° 30’E. The detector was lowered once with  $S = 7.44$  m (“1.13 M $\Omega$ ” gain) at 1000 m depth and a second time with  $L = 40.37$  m (“open” gain) at 1000 m, 3500 m and 3900 m depth. The sea had a depth of about 4160 m. The drift of the ship was less than 0.2 knots.

Location “c”: 36° 34’N; 21° 36’E. The detector was lowered twice down to a maximum depth of 3500 m, the first time with  $S = 7.44$  m (“1.13 M $\Omega$ ” gain) and the second with  $L = 20.69$  m (“open” gain). The sea had a depth of about 3600 m. The drift of the ship was less than 0.5 knots.

For each set of data, the distribution of the peak-voltage of the received pulses is plotted; typical distribution is shown in Fig. 4. Some of these distributions have a low tail. This tail is caused by the tilt and rotation of the light source and photodetector resulting to a loss of detected light intensity [4]. In order to minimize this effect the analysis was done by rejecting this tail. Since there is no rigorous way of defining this tail, the analysis was done as follows: the highest 40% of the measurements of a particular data set was taken and the mean and the standard deviation of this sample was calculated. Then only those of the original measurements that were within two standard deviations from this mean were kept. The error  $\delta\beta$  was calculated taking in account the effects of the error of the peak-voltage of each set of data, the error of the calibration curves and the error in the measurements of the distances

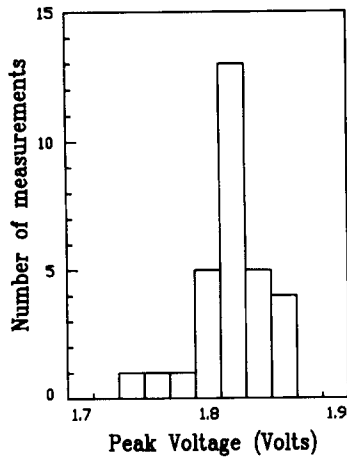


Fig. 4. Typical peak-voltage distribution of the received pulses of a set of data.

$L$  and  $S$  ( $\pm 0.01$  m). The main contribution comes from the first error and most of it is statistical. The results are summarized in Table 1 and plotted in Fig. 5.

The relative contribution of errors and uncertainties to a sample of calculated values of  $\beta$  are shown in Table 2.

The statistical errors on the  $1/e$  transmission distance  $\beta$  is less than 20% (at location “b” and depths 3500 m

Table 1  
Values of  $1/e$  transmission distance at various depths

Location	Sea bottom (m)	Depth (m)	$\beta$ (m)
a	3730	200	$40 \pm 8$
		1000	$52 \pm 11$
		2000	$52 \pm 11$
		3000	$52 \pm 11$
		3500	$52 \pm 10$
		3650	$54 \pm 11$
b	4160	1000	$52 \pm 10$
		3500	$55 \pm 17^a$
		3900	$62 \pm 22^a$
c	3600	100	$36 \pm 6$
		1000	$58 \pm 13$
		2000	$45 \pm 8$
		3000	$46 \pm 8$
		3500	$52 \pm 6$

<sup>a</sup> Due to ship scheduling, there was sufficient time, for those two depths, to take measurements only with the long cable (40.37 m). The  $1/e$  transmission distance  $\beta_x$  at a depth  $D_x$  is calculated from Eq. (1), using the  $1/e$  transmission distance  $\beta_{1000m}$  measured at a depth  $D_{1000m}$

$$\beta_x = L / (\ln I_{1000m} / I_x + L / \beta_{1000m}), \quad (3)$$

where  $I_{1000m}$  and  $I_x$  are the light intensities detected by the photodetector at the depths  $D_{1000m}$  and  $D_x$  and  $L$  the distance between the light source and the photodetector.

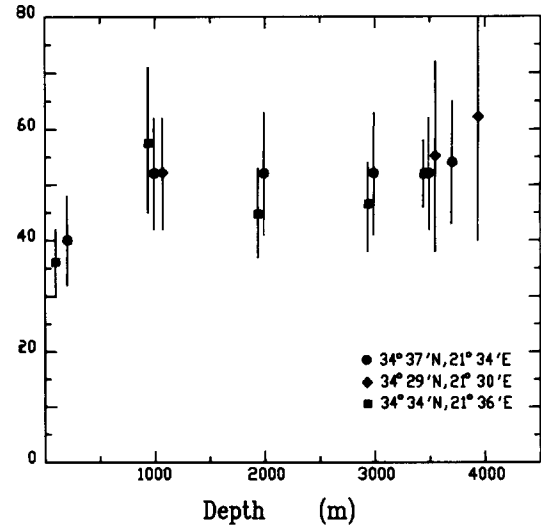


Fig. 5.  $1/e$  transmission distance versus depth at three locations near the future NESTOR site.

Table 2  
Relative contribution of errors to the value of  $\beta$  ( $\delta\beta/\beta$ )

Location	a	a	c	c
Depth (m)	3500	3650	3000	3500
Error in the measurement of $S$	$< \pm 1\%$	$< \pm 1\%$	$< \pm 1\%$	$< \pm 1\%$
Error in the measurement of $L$	$< \pm 1\%$	$< \pm 1\%$	$< \pm 1\%$	$< \pm 1\%$
Pulse to pulse variation on $I_S$	$\pm 3\%$	$\pm 3\%$	$\pm 4\%$	$\pm 5\%$
Pulse to pulse variation on $I_L$	$\pm 9\%$	$\pm 19\%$	$\pm 5\%$	$\pm 8\%$
Calibration uncertainty on $I_S$	$\pm 2\%$	$\pm 2\%$	$\pm 6\%$	$\pm 7\%$
Calibration uncertainty on $I_L$	$< \pm 1\%$	$< \pm 1\%$	$< \pm 1\%$	$< \pm 1\%$

and 3900 m, the error is larger, since in those points  $\beta$  was calculated using Eq. (3), Table 1).

## 5. Conclusions

The sea-water at the depths where NESTOR will be deployed has a high light transmissivity. The measurements show on average a  $1/e$  transmission distance better than 50 m, from a depth of 3000 m down to 4000 m. Averaging the data for depths greater than 3500 m, it is found that the  $1/e$  transmission distance is  $55 \pm 10$  m.

The attenuation coefficient was measured, in the same general location, with 47 water samples taken from various depths during the “Academic Mstislav Keldish” cruise [5] and during a previous cruise in 1985 [6]. For those measurements a monochromator–photometer with a well collimated light beam (collimation better than 30 arcmin) was used. It was found that the light attenuation coefficient at a typical wavelength, e.g. 460 nm wavelength, is between

$0.025 \text{ m}^{-1}$  and  $0.045 \text{ m}^{-1}$  (i.e. attenuation lengths between 43 m and 23 m) at depths deeper than 3000 m.

Those measurements with the sharply collimated beam lose most of the scattered light while our experiment, being a poor geometry experiment, detects most of it. So the measurements with the two geometries are compatible only in very clear water where the scattering is small.

### Acknowledgements

We would like to thank for their valuable assistance V. Alboul and his team in deploying the detector and P. Preve in the data acquisition. Also we would like to thank Deep Sea Power and Light, USA for their advice and help in preparing the instrument.

### References

- [1] L.K. Resvanis et al., NESTOR, a neutrino particle astrophysics underwater laboratory for the mediterranean, High Energy Neutrino Astrophysics Workshop, Hawaii, March 1992, ed. V.J. Stenger.
- [2] DUMAND II, proposal to construct a deep-ocean laboratory for the study of high energy neutrino and astrophysics particle physics, HDC-2-88, August 1988, Hawaii DUMAND Center, University of Hawaii.
- [3] N.G. Jerlov, Optical Oceanography (Elsevier, 1968).
- [4] Bradner and G. Blackinton, Appl. Opt. 23 (1984) 1009.
- [5] S.A. Khanaev and A.F. Kuleshov, Proc. 2nd NESTOR Int. Workshop, ed. L.K. Resvanis, 1993, p. 253.
- [6] G.S. Karabashev and A.F. Kuleshov, Dokl. Akad. Nauk. USSR 298(2) (1988) 467.